COMPLEX CRATER FORMATION: INSIGHTS FROM COMBINING OBSERVATIONAL CONSTRAINTS WITH NUMERICAL MODELS OF THE WEST CLEARWATER IMPACT STRUCTURE.

A. S. P. Rae[1*], J. V. Morgan[1], G. S. Collins[1], G. R. Osinski[2] and R. A. F. Grieve[2], [1]Impacts and Astromaterials Research Centre, Department of Earth Science and Engineering, Imperial College London, SW7 2BP, UK, a.rae14@imperial.ac.uk, [2]Department of Earth Sciences, University of Western Ontario, London, ON, Canada, N6A 5B7

Introduction: A significant, and transient, reduction in the strength of target rocks is required to form complex craters. One of the working hypotheses to explain this weakening, often adopted in numerical impact simulations, is acoustic fluidisation [1]. This mechanism supposes that the passage of the shock wave and subsequent deformation causes vibrations that are sufficiently strong to release overburden pressure on slip surfaces, therefore weakening the material whilst vibrations occur. The parameters of the full acoustic fluidisation model and the related block-oscillation model [2] are poorly constrained.

Here direct observations from the West Clearwater impact structure are used to constrain the parameters of the acoustic fluidisation model. This has been achieved by comparing shock barometry, drill core logs and other geological observations with the results of numerical simulations.

Located in northern Quebec, Canada (56°13'N, 74°30'W), West Clearwater Lake is generally considered to be a 32-km diameter peak-ring impact structure. It is a well-exposed, relatively well-preserved structure that had a simple pre-impact target. Five drill cores were recovered from the structure by the Dominion Observatory (now Natural Resources Canada) during the mid-1960s [3].

Methods: A field campaign was carried out in the summer of 2014, comprising geological mapping and sample collection. In addition, the five recovered drill cores, currently housed in Ottawa, were logged and petrographically analysed. Petrographic analysis included universal-stage measurements of planar deformation features (PDFs) in quartz to obtain shock pressure estimates of the para-autochthonous lithologies. PDFs were indexed using ANIE [4] and assigned shock pressures based on [5, and refs therein].

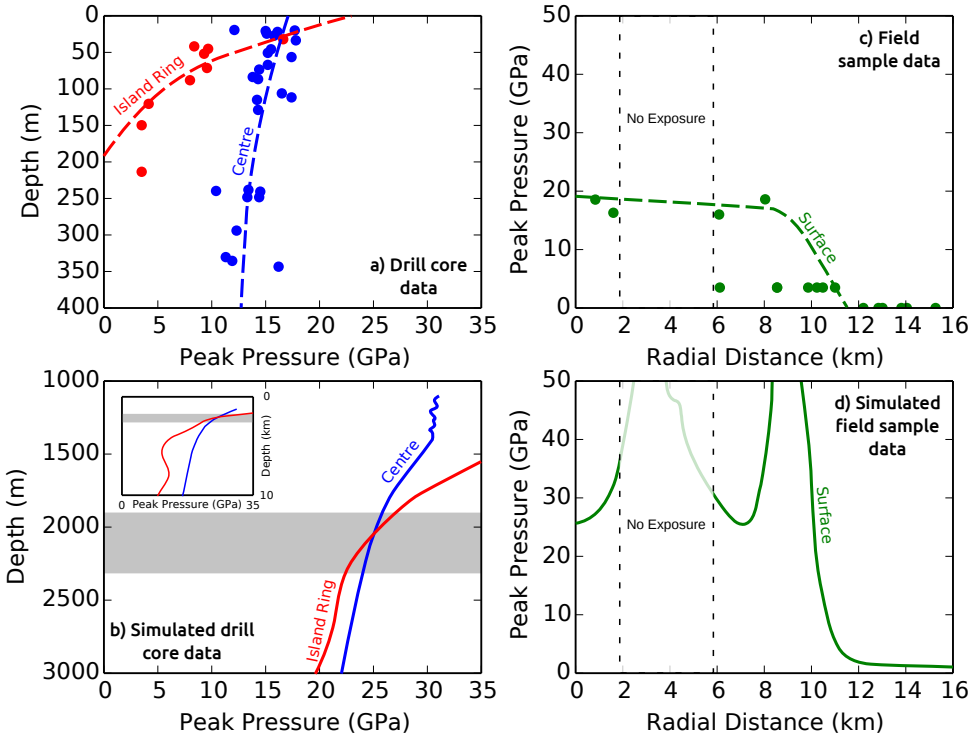

Figure 1: a) Assigned shock pressure with depth in drill cores. b) Simulated drill cores corresponding to the cores in a), inset, shock pressure with depth over 10 km, highlighted region indicates the comparable area of the simulated drill core. c) Assigned shock pressure with radial distance in surface samples. d) Simulated slice through the model, at the top of the highlighted region in b).

In parallel to this, numerical simulations were carried out using the iSALE shock physics code [6, and refs therein]. The parameters of both the full acoustic fluidisation model and the block oscillation model were investigated to determine their effect on the distribution of peak shock pressure and final crater form.

Results: Field mapping and drill core logs at West Clearwater indicate that the stratigraphic level of the para-autochthonous crater floor is near present day lake-level. The topography (125m) of the island ring is largely composed of the remnant impact melt-sheet. Deformation due to crater collapse is pervasive and occurs as thin, frequently spaced (1–10m) shear bands, melt veins, and occasional breccias, often with little apparent displacement. We found no evidence to support the presence of large "interblock breccias", which are assumed and required in the block model hypothesis.

Shock barometry (Table 1) of drill cores from West Clearwater show a rapid attenuation of shock beneath the island ring and a low attenuation of shock beneath the central islands. Both cores approach similar shock values at the surface. Surface samples also show that shock level is fairly constant across the uplifted region (Figure 1).

Numerical modelling of the West Clearwater impact event produces a spatial shock distribution pattern consistent with the observed pattern despite discrepancies between absolute values (Figure 2).

Summary: Our results demonstrate that the rheology of an acoustically fluidised mass is capable of producing spatial shock distributions consistent with the observed shock distribution at the West Clearwater impact structure. Moreover, using observed shock distribution to constrain the target rheology appears to be a promising approach for understanding complex crater formation.

Although the block model adequately produces a viable rheology for crater collapse, observational evidence to support the physical justification of the block model is lacking. This may favour the use of the full acoustic fluidisation model in crater collapse simulations.

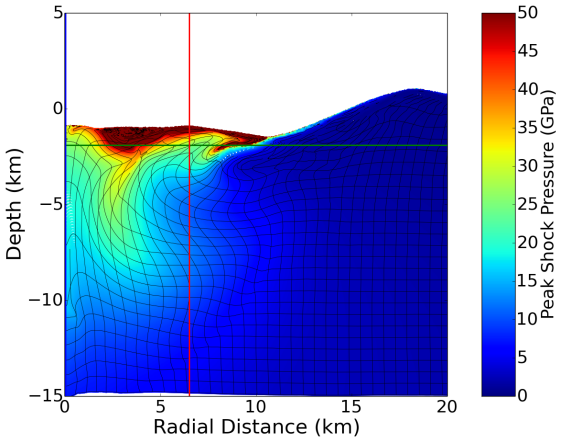

Figure 2: Final shock distribution pattern in an iSALE simulation of the West Clearwater structure. Coloured vertical and horizontal lines indicate the position of simulated drill-cores and slices seen in Figure 1.

Acknowledgments: ASPR acknowledges the assistance of the UWO team; R. Wilks, M. Kerrigan, R. Misener, A. Coulter, and D. Saint-Jacques along with NASA FINESSE. We gratefully acknowledge the developers of iSALE (www.isale-code.de). This work was funded by STFC.

References: [1] Melosh, H. J. (1979) *Journal of Geophysical Research 84*, 7513-7520 [2] Ivanov, B. A. and Kostuchenko V. N. (1997) LPS XXVIII, Abstract #631 [3] Grieve R. A. F. (2006) Impact Structures in Canada, *St Johns: Geological Association of Canada* [4] Huber M. S. et al. (2011) *Meteoritics and Planetary Science 46*, 1418-1424 [5] Stöffler D. and Langenhorst F. (1994) *Meteoritics 29*, 155-181 [6] Wünnemann K. et al. (2006) *Icarus 180*, 514-52.

Samples	Number of measured sets	Number of indexed PDFs	Unindexed %	Number of quartz grains (n)
53	1958	1668	14.8	1516

No. of PDF sets, % relative to n

0	1	2	3	4
34.5	17.9	32.8	13.5	1.3

Indexed plane abundance (absolute frequency %)

c (0001)	ω ($10\bar{1}3$)	Π ($10\bar{1}2$)	r, z ($10\bar{1}1$)	m ($10\bar{1}0$)	ξ ($11\bar{2}2$)	s ($11\bar{2}1$)	ρ ($21\bar{3}1$)	x ($51\bar{6}1$)	a ($11\bar{2}0$)	($22\bar{4}1$)	($31\bar{4}1$)	t ($40\bar{4}1$)	k ($51\bar{6}0$)	e ($10\bar{1}4$)
27.9	29.1 (+ 4.7)	6.0	2.7	0.7	2.6	1.4	2.3	2.4	0.3	0.9	1.8	0.9	1.1	15.3

Table 1: Summary of all universal-stage results collected at the time of writing, Indexed plane abundance, given in absolute frequency percent, does not include unindexed PDFs. PDF sets in overlap between $(10\bar{1}3)$ and $(10\bar{1}4)$ were assigned the $(10\bar{1}3)$ orientation indicated by the bracketed value. A 5° error envelope was used to assign PDFs.